
AMICABLE AID: TURNING ADVERSARIAL ATTACK TO BENEFIT CLASSIFICATION

Juyeop Kim
Yonsei University
j2kymusic@yonsei.ac.kr

Jun-Ho Choi
Yonsei University
idearibosome@yonsei.ac.kr

Soobeam Jang
Yonsei University
soobeam.jang@yonsei.ac.kr

Jong-Seok Lee
Yonsei University
jong-seok.lee@yonsei.ac.kr

ABSTRACT

While adversarial attacks on deep image classification models pose serious security concerns in practice, this paper suggests a novel paradigm where the concept of adversarial attacks can benefit classification performance, which we call *amicable aid*. We show that by taking the opposite search direction of perturbation, an image can be converted to another yielding higher confidence by the classification model and even a wrongly classified image can be made to be correctly classified. Furthermore, with a large amount of perturbation, an image can be made unrecognizable by human eyes, while it is correctly recognized by the model. The mechanism of the amicable aid is explained in the viewpoint of the underlying natural image manifold. We also consider universal amicable perturbations, i.e., a fixed perturbation can be applied to multiple images to improve their classification results. While it is challenging to find such perturbations, we show that making the decision boundary as perpendicular to the image manifold as possible via training with modified data is effective to obtain a model for which universal amicable perturbations are more easily found. Finally, we discuss several application scenarios where the amicable aid can be useful, including secure image communication, privacy-preserving image communication, and protection against adversarial attacks.

1 Introduction

Deep learning technologies have been widely expanded to various applications thanks to the abundance of data and computational resources. On the other hand, recent studies have shown that deep neural networks are highly vulnerable to *adversarial attacks*, which fool the target deep model by adding imperceptible noise to input images. For instance, adversarial attacks can make image classification models misclassify a given image [1]. Such *vulnerability* against adversarial attacks raises significant security concerns in real-world applications [2].

An attack can be defined as adding perturbation δ to image x to mislead an image classification model. There are two natures that make this an “attack” [4]. First, δ should be obtained so that the model does not recognize the image as a ground-truth class y (i.e., *deterioration*). Second, δ should be small enough to conceal the fact that the original image has been manipulated (i.e., *inconspicuousness*).

A question that motivated our work in this paper is as follows: *If it is possible to find a perturbation that can deteriorate classification performance, will it be also possible to find a perturbation that can improve classification performance?* We find that the answer is yes and doing so is surprisingly effective. Figure 1 shows that adding an imperceptible perturbation pattern to an image can not only increase the confidence score when the original classification result is correct (Figure 1(a)) but also make the classification result correct even if the model misclassifies the original image (Figure 1(c)). More surprisingly, it is also possible to add a significant amount of perturbation to increase confidence or fix the classification result so that the original content is completely destroyed (Figures 1(b) and 1(d)). We call this phenomenon as **amicable aid** as an opposite concept to adversarial attack. We can rethink the role

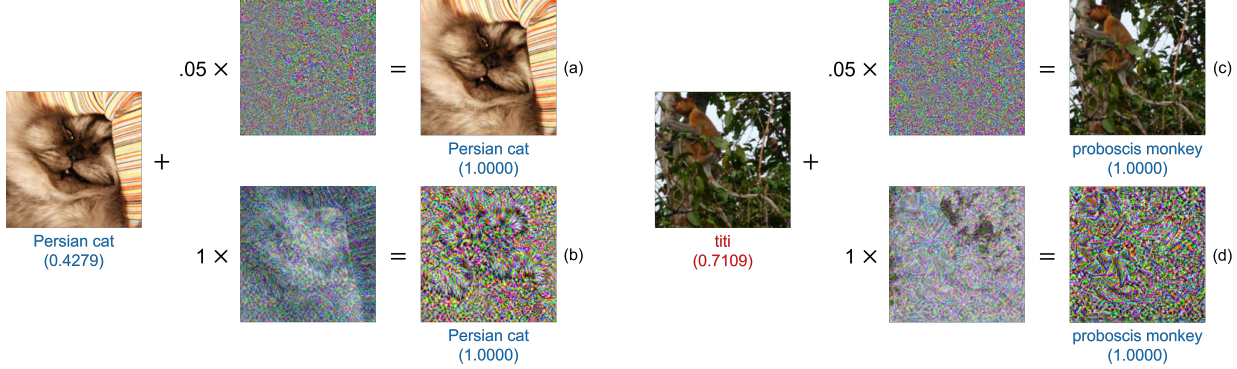


Figure 1: Concept of the proposed amicable aid. (Left) The original image is correctly classified as “Persian cat” by the trained VGG16 [3] model with a confidence of 0.4279. (a) By adding a small perturbation computed by our method, called weak aid, the confidence can be maximized. (b) Confidence boosting can be obtained even with a large amount of perturbation that completely destroys the original content, called strong aid. (Right) The original image (“proboscis monkey”) is misclassified by VGG16 as “titi.” (c) By the weak aid, the image can be correctly classified with the maximum confidence. (d) The strong aid also can change the image in a way that it is correctly classified with the maximum confidence.

of image perturbations that have been used for adversarial attacks based on the two natures, i.e., deterioration and inconspicuousness.

In this paper, we define the notion of amicable aid and perform analysis regarding its characteristics and mechanism. We show that the amicable aid can be performed with high success rates by iterative gradient-based search where the search direction is made opposite to conventional adversarial attacks. We also define the weak amicable aid with imperceptible perturbations and the strong amicable aid with perceptible perturbations destroying the original image content. We explain the mechanism of the amicable aid in the viewpoint of image manifold and decision boundary. This view also explains enhanced robustness of images containing amicable perturbations against adversarial attacks. We also present further analysis results to understand models’ prediction under the amicable aid and to examine transferability of amicable perturbations. Then, we examine the feasibility of finding universal perturbations of the amicable aid. We show that while finding a universal perturbation is challenging, the challenge can be resolved by making the decision boundaries more perpendicular to the data manifold. Finally, we discuss some potential real-world applications where the amicable aid can be useful.

2 Related work

2.1 Adversarial attacks

Recent studies have shown that many deep learning-based image classification models are highly vulnerable to malicious image manipulation, which is known as the adversarial attack. In [5], it was shown that a hardly imperceptible perturbation added to an image can make a classification model produce an incorrect classification result. A strong attack method called fast gradient sign method (FGSM) was developed in [2], which calculates a perturbation from the sign of the gradients in the classifier. An iterative version of FGSM (called I-FGSM) was proposed in [6], which achieved higher attack performance than FGSM. Several other adversarial attack techniques have been proposed with various perspectives and objectives [7, 8, 9, 10, 11, 12, 13]. In addition to these white-box attacks, there exist black-box attack approaches that do not assume complete availability of the knowledge regarding the target classifier, e.g., [14, 15]. Existence of an image-agnostic universal perturbation has been also shown [16], i.e., a single perturbation can attack multiple images.

A plausible explanation of adversarial attacks is the manifold theory. While natural images lie on a low-dimensional data manifold, adding an adversarial perturbation to an image causes the image to leave the manifold and also cross the decision boundary. In this sense, attacks adding noise-like perturbations can be called *off-manifold* attacks, whereas *on-manifold* adversarial samples remain on the manifold with preserving visual naturalness [17, 18]. Finding off-manifold samples becomes easy when the decision boundary lies close to the manifold [19].

2.2 Applications of adversarial attacks

While adversarial attacks are undesirable threats for classifiers in general, there have been a few attempts to exploit attacks for specific purposes recently. The work in [20] used a set of adversarial examples as a fingerprint of a deep neural network in order to deal with model stealing. In [21], it was found that model training using attacked images can improve generalization performance via regularization. In [22], an adversarial attack was used to explain learned representations.

To the best of our knowledge, the work [23] is the only attempt to search a perturbation minimizing the classification error. This work proposed a method to protect privacy by making an image unlearnable with a perturbation during model training. This method and ours commonly set the direction for searching perturbations to the opposite of that of adversarial attacks. However, the former aims to fool the training process, whereas our work focuses on understanding and analyzing the characteristics and mechanism of error-minimizing perturbations in the viewpoint of improving classification performance.

3 Amicable aid

3.1 Method

Given an image classification model with weight parameters θ and an image x with the true class label y , performing the amicable aid can be formulated as an optimization problem as follows:

$$\begin{aligned} & \min_{\delta} J(x + \delta, y, \theta) \\ & \text{such that } \|\delta\|_p \leq \epsilon, \end{aligned} \quad (1)$$

where δ is the perturbation, J is the cost function (e.g., cross-entropy), and ϵ is a hyperparameter. In other words, we want to find δ that minimizes the cost function while its p -norm is bounded by ϵ . Note that this formulation is exactly the opposite to that for adversarial attacks where minimization is replaced by maximization.

Many of gradient-based adversarial attack methods can be adopted to solve the above optimization problem. For instance, the idea of FGSM [2], which is one of the most popular and strongest attacks, can be used for $p = \infty$:

$$\delta = -\epsilon \cdot \text{sign}(\nabla_x J(x, y, \theta)). \quad (2)$$

Note that the negative signed gradient is used here as opposed to the FGSM attack. It is known that FGSM can be made more powerful using an iterative approach, I-FGSM [6]. Similarly, an iterative version of (2) can be formulated as follows.

$$x_0 = x, \quad (3)$$

$$\tilde{x}_{n+1} = \text{clip}_{0,1}\left(x_n - \frac{\epsilon}{N} \text{sign}(\nabla_x J(x_n, y, \theta))\right), \quad (4)$$

$$x_{n+1} = \text{clip}_{-\epsilon, \epsilon}(\tilde{x}_{n+1} - x) + x, \quad (5)$$

where N is the number of iterations and $\text{clip}_{a,b}(z) = \min(\max(z, a), b)$.

As shown in Figure 1, ϵ can be controlled so that the perturbation becomes either imperceptible with a small ϵ (Figures 1(a) and 1(b)) or perceptible with a large ϵ (Figures 1(b) and 1(d)), which we call **weak aid** and **strong aid**, respectively¹. While only small values of ϵ are meaningful in the case of adversarial attacks in order to effectively conceal perturbations, the strong aid with a significant amount of perturbation that completely destroys the original content is not only interesting but also useful in some applications (see Section 5).

We apply the weak and strong aid to the test set of CIFAR-100 [24]. Three models, namely, VGG16 [3], ResNet50 [25], and MobileNetV2 [26], are employed. We use $\epsilon = .05$ for the weak aid and $\epsilon = 5$ for the strong aid. The number of iterations (N) is set to 50. The results are shown in Table 1. It is observed that the aids significantly improve the classification performance, showing near-perfect or perfect classification accuracies and confidence scores. Moreover, finding perturbations for the strong aid seems slightly more difficult compared to the weak aid due to the requirement of large perturbation changes at each search iteration.

¹The I-FGSM-based amicable aid have an advantage that we can accurately control the amount of perturbation; an appropriate value of ϵ for a weak or strong aid can be intuitively determined. While we found that the C&W-based aid is also successful, controlling the strength of the aid through the balancing hyperparameter is not straightforward.

Table 1: Classification accuracy (with average confidence for the true class labels) for the original images, weakly aided images, and strongly aided images for CIFAR-100.

	VGG16	ResNet50	MobileNetV2
Original	72.32% (.7090)	78.82% (.7574)	68.90% (.6182)
Weak aid	100.0% (1.000)	100.0% (1.000)	99.88% (.9954)
Strong aid	97.22% (.9638)	99.42% (.9905)	93.83% (.9197)

3.2 Mechanism

In the manifold-based explanation for adversarial attacks, ordinary adversarial attacks that modify images in unnatural ways cause the images leave the manifold [17]. The mechanism of the amicable aid can be also explained in the viewpoint of the manifold and decision boundary, as illustrated in Figure 2. The original image (α), which is inside the decision boundary and thus correctly classified, lies on the manifold. By an off-manifold attack, it leaves the manifold and also goes beyond the decision boundary so that the classification result becomes wrong (α'). Amicable aids also make the image leave the manifold, but the perturbed images (β and γ) still stay within the decision region. The strongly aided image (γ) is located farther from the manifold due to a larger amount of perturbation by a large value of ϵ than the weakly aided image (β) using a small value of ϵ .

To support this explanation, we check the distance of aided images from the manifold. The true manifold is not known, thus it is approximated by the nearest neighbor-based method described in [17]. Figure 3 shows the average distance of the aided images to the approximated manifold with respect to the value of ϵ for the CIFAR-100 test images when VGG16 is employed. It is clearly observed that the distance to the manifold increases as ϵ increases.

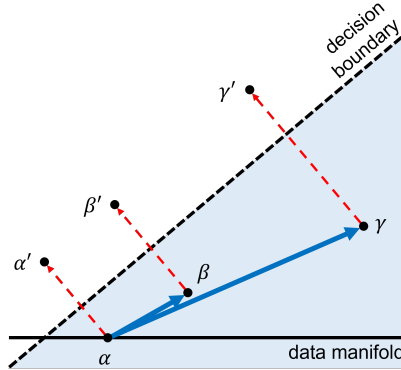


Figure 2: Illustration of the process of the amicable aid. α indicates the original image residing on the manifold. The blue solid arrows mean modification processes of the original image by the amicable aid, while the red dashed arrows mean modification processes by the attack. β and γ correspond to a weakly and strongly aided images, respectively. Both attack and aid make the original image leave the manifold, but the aided images still remain inside the decision region (shaded region) while the attacked images do not.

3.3 Enhanced robustness

Since the amicable aid searches a perturbation in the opposite direction of an adversarial attack, a naturally arising question is: *Will the aided images be more robust to adversarial attacks than their original counterparts?* To answer this question, the classification accuracy before and after an adversarial attack is examined for the correctly classified images by VGG16. As an adversarial attack, we employ I-FGSM with $\epsilon_{\text{attack}} = .01$ and $.05$ and a number of iterations of 50.

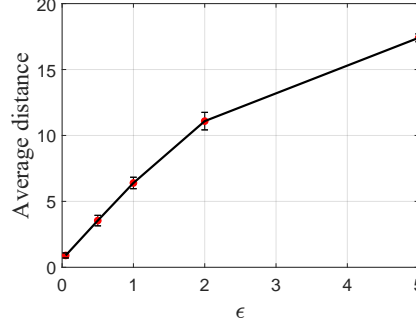


Figure 3: Average distance from the aided images to the approximated manifold with respect to the value of ϵ .

The results are shown in Table 2. It is clearly observed that the weak and strong aids improve robustness against the attacks. In particular, the strongly aided images show significantly enhanced robustness, e.g., from 24.10% to 90.70% for $\epsilon_{\text{attack}} = .01$. These results can be explained from Figure 2. An aid tries to maximize the confidence for the given image, i.e., the image moves *deeper* in the decision region and becomes farther from the decision boundary. As a result, the aided image becomes harder to attack.

Table 2: Classification accuracy (with average confidence for the true class labels) for CIFAR-100 with VGG16 when aided images are attacked by I-FGSM with $\epsilon_{\text{attack}} = .01$ or $.05$. Note that we use only correctly classified images before the attack in each case, so the accuracies of unattacked images are all 100%.

	Unattacked	$\epsilon_{\text{attack}} = .01$	$\epsilon_{\text{attack}} = .05$
Original	100.0% (.9589)	24.10% (.2326)	1.83% (.0139)
Weak aid	100.0% (1.000)	45.75% (.4538)	2.11% (.0171)
Strong aid	100.0% (.9881)	90.70% (.8904)	28.84% (.2780)

3.4 Analysis

The strong aid completely distorts an image so that the image becomes unrecognizable for human eyes (Figures 1(b) and (d)). The model, however, still classifies it surprisingly well. Then, *which image region does the model attend to make such a decision?* To answer this question, we use the Grad-CAM method [27] to examine important regions for decision in aided images. Figure 4 compares the Grad-CAM results of the original image from the ImageNet dataset, weakly and strongly attacked images by I-FGSM, and weakly and strongly aided images for VGG16. The attended regions in the attacked images are mostly deviated from those in the original images. However, in the case of the aided images, the originally attended regions are still attended, which surprisingly holds even in the case of the strong aid. It seems that perturbations are added in such a way that important image features are intact by the aid but effectively destroyed by the attack. Figure 5 compares the distribution of the intersection over union (IoU) between the attended regions in the original images and perturbed images. It is apparent that there exist larger overlaps in the attended regions between the original and aided images than between the original and attacked images.

3.5 Transferability

In adversarial attacks, the *transferability* means the possibility that an adversarial example causing misclassification for one model is also misclassified by another model [28]. The concept of transferability can be also applied to the amicable aid, i.e., we want to examine if aided examples found for one model are transferable to different models. A transferable aided example will be correctly classified by several models without necessity of crafting a new aided example for each model.

Table 3 summarizes transferability of aided images from CIFAR-100 among VGG16, ResNet50, and MobileNetV2. The weak aid is highly transferable across the models, whereas the strong aid is not. A weakly aided example for a

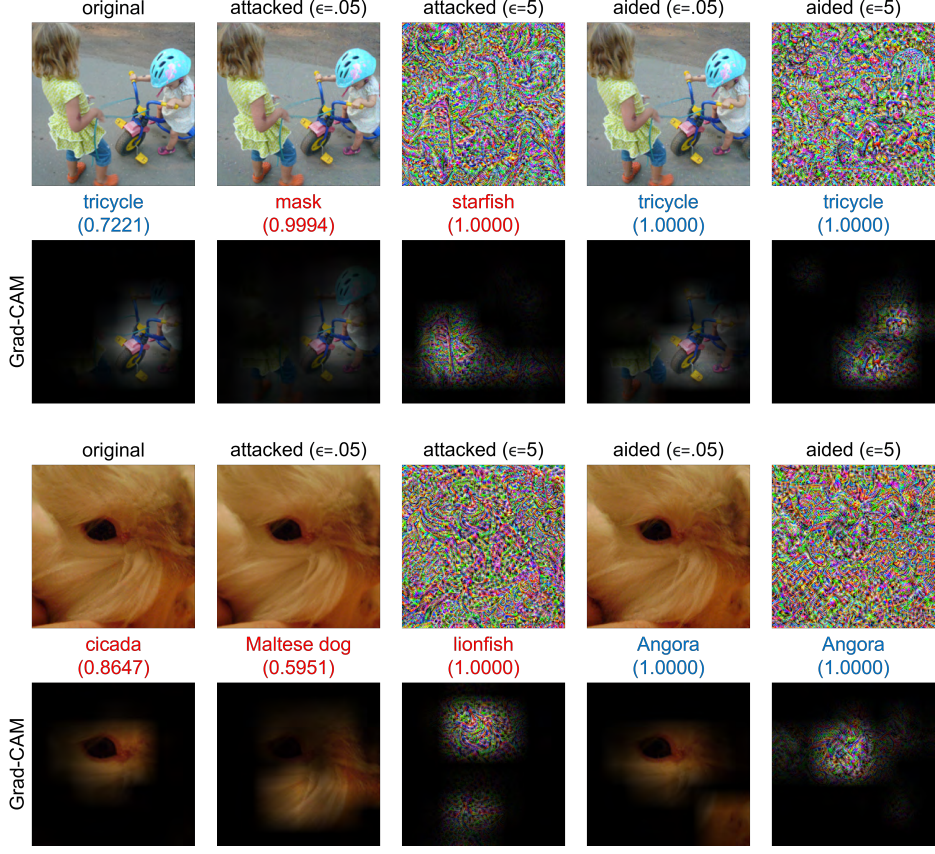


Figure 4: Grad-CAM results of the original, attacked, and aided images from the ImageNet validation set, where VGG16 is employed. Predicted class labels and confidence scores are also shown in blue (for correct classification) or red (for misclassification).

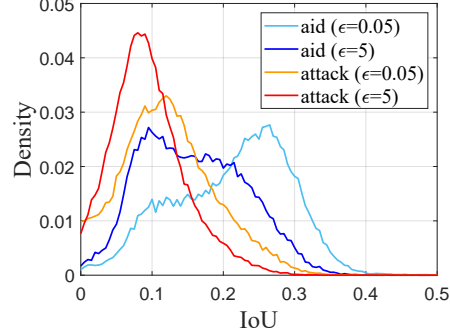


Figure 5: Distribution of the intersection over union (IoU) of the attended regions between the original and aided/attacked images.

model leaves the data manifold by a relatively small distance. Thus, with high probability it remains inside the decision region of another model. On the other hand, the strong aid for a model makes an image move relatively far from the manifold until the point that is inside the decision region of the model but outside the decision region of another model.

4 Universal amicable aid

In adversarial attacks, it is possible to find an image-agnostic perturbation that affects multiple images to make a given model misclassify them, which is known as the universal attack [16]. Borrowing this idea, the concept of *universal*

Table 3: Transferability of amicable aids in terms of classification accuracy of weakly or strongly aided images from CIFAR-100 when a model in a row is used to obtain aided examples and the model in a column performs classification using the examples.

		VGG16	ResNet50	MobileNetV2
VGG16	weak	100.0%	86.78%	75.63%
	strong	97.22%	1.13%	1.51%
ResNet50	weak	87.64%	100.0%	81.94%
	strong	5.57%	99.42%	1.93%
MobileNetV2	weak	86.38%	89.76%	99.88%
	strong	1.93%	1.04%	93.83%

amicable aid can be proposed. The objective of the universal amicable aid is to find an image-agnostic perturbation that can aid multiple images to obtain correct classification results, which is expected to be a more challenging problem than the universal attack, as illustrated in Figure 6. In this section, we explore the feasibility of the universal amicable aid.

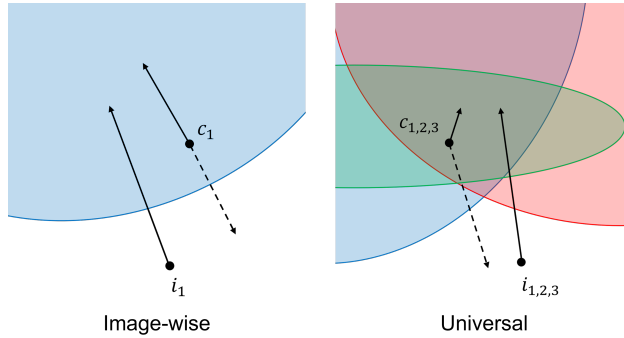


Figure 6: Illustration of the image-wise aid and the universal aid (solid lines). A shaded region represents the decision region where a correct classification result is obtained. The image-wise attack and the universal attack are also shown (dotted lines) for comparison. (Left) An original image (c_1) that is correctly classified is moved within the decision region by the amicable aid. An image (i_1) that is misclassified is moved into the decision region by the amicable aid. (Right) Three correctly classified images (c_1, c_2 , and c_3) are super-imposed and their corresponding decision regions are shown with different colors. The universal amicable aid (solid line) needs to move the three images within the intersection of the three decision regions. Three misclassified images (i_1, i_2 , and i_3) also need to be sent inside the intersection by the universal aid. On the other hand, the universal attack (dotted line) needs to move three images outside their decision regions, where the region of the valid universal attack is far wider than that of the universal aid.

4.1 Finding universal perturbations

Basically, a universal amicable perturbation for aid can be found in a way similar to that for finding a universal adversarial perturbation, i.e., using the average gradient over multiple images in (4). There are several questions related to the existence of universal amicable perturbations:

- Does a universal perturbation exist for a certain amount of images?
- Is the found universal perturbation effective for both strengthening the confidence of correctly classified images and making misclassified images being correctly classified?
- Is the found universal perturbation applicable to unseen data?

In order to systematically deal with these questions, we conduct the following experiment. To observe the behavior of the universal amicable aid for correctly and incorrectly classified images, we form two sets referred to as `correctA` and `incorrectA`. Each dataset consists of 1,000 images from CIFAR-100 that are originally classified correctly and incorrectly by VGG16, respectively. `correctA`, `incorrectA`, and the aggregation of the two sets (i.e., `correctA+incorrectA`) are used to find universal amicable perturbations. The found universal perturbations are

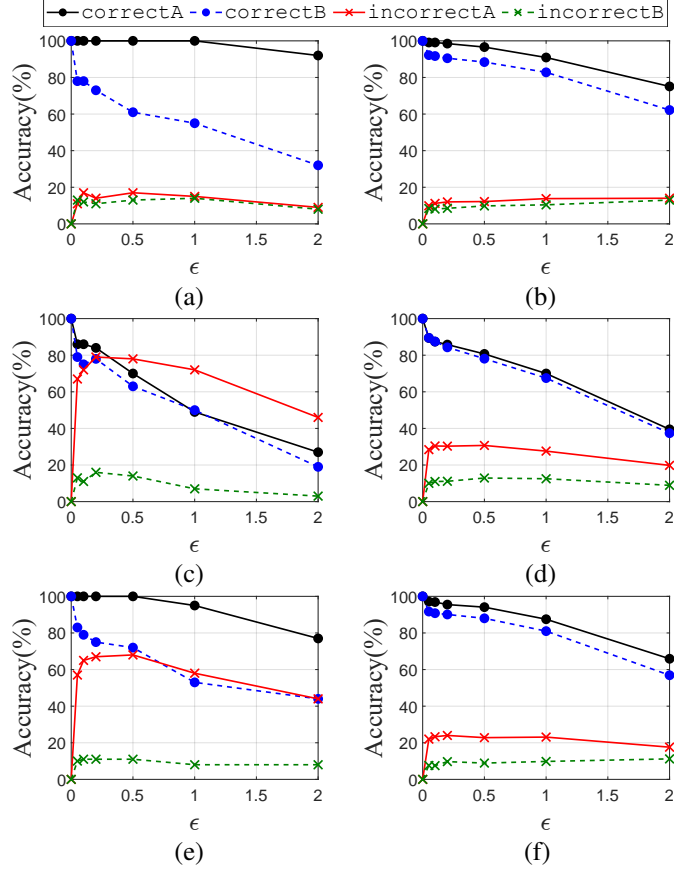


Figure 7: Classification accuracy of four different image sets when universal amicable aids are applied. Universal perturbations are found from and applied to 100 images (left column) or 1,000 images (right column) of **correctA** (top row), **incorrectA** (middle row), or **correctA+incorrectA** (bottom row).

applied to themselves (i.e., **correctA** and **incorrectA**), and also tested on another two sets formed similarly, which are referred to as **correctB** and **incorrectB**, respectively, to evaluate generalization performance of the universal amicable perturbations for unseen data.

Figure 7 summarizes the experimental results over different values of ϵ . The figure shows the accuracy for the universally aided datasets (**correctA**, **correctB**, **incorrectA**, and **incorrectB**) when universal amicable perturbations are found using 100 or 1,000 images in **correctA**, **incorrectA**, or **correctA+incorrectA**. From the results, following observations can be made. (1) For correctly classified images, universal perturbations are successfully found when they are obtained from correctly classified images. Those obtained using 1,000 images especially show reasonable generalization performance (Figure 7(b)). However, there also exist accuracy drops for large values of ϵ . For incorrectly classified images, about 10% to 15% are made correctly classified by the perturbations, which is thought as a result of leaving the data manifold and entering the correct decision regions for these images. (2) Finding universal perturbations using incorrectly classified images is challenging. When only 100 images are used (Figure 7(c)), the universal perturbations found for **incorrectA** can significantly improve the accuracy for the same dataset; however, for 1,000 images (Figure 7(d)), the accuracy for **incorrectA** drops significantly and the perturbations do not generalize well on **incorrectB**. (3) When both **correctA** and **incorrectA** are used to find universal perturbations, the perturbations work as almost well as those found from each set, but accuracy drops are also observed for large ϵ values (Figures 7(e) and (f)).

The results show that it is feasible to find a universal perturbation for the weak aid, but it is challenging for the strong aid. For success of the universal amicable aid, the same perturbation must allow all images to stay in their own decision regions, which is particularly challenging for a large value of ϵ , as shown in Figure 6.

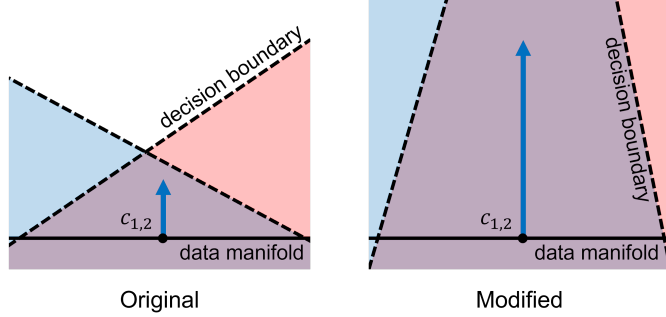


Figure 8: Illustration of the universal aid for an ordinary model and a model trained on a modified dataset. Two correctly classified images (c_1 and c_2) are super-imposed and their corresponding decision regions are shown with different colors. A straight line represents the data manifold where the natural images reside while dotted lines represent the decision boundaries. (Left) A universal aid cannot make the two images go beyond the intersection of the decision boundaries. (Right) A dataset containing modified images is used to train a model so that the decision boundaries have larger angles with the data manifold, which expands the intersection of the decision regions and thus allows the universal aid to be successful with a higher strength.

4.2 Improving universal aid

Will it be possible to improve the universal aid, i.e., to find amicable perturbations having large values of ϵ and showing good generalization performance on unseen images? Such improvement can be useful for some applications where the image-specific aid is not applicable but fixed universal amicable perturbations needs to be used (see Section 5). An idea to achieve this is illustrated in Figure 8. If we can make the decision boundaries perpendicular to the data manifold, more (correctly classified) images can leave the data manifold by a larger distance while they still remain inside their decision regions. To realize this, we employ the data modification method presented in [29]. In this method, the data for model training are modified to contain noise in the normal direction of the data manifold by performing principal component analysis (PCA) and then adding noise, so that the model learns decision boundaries perpendicular to the data manifold. Algorithm 1 summarizes the procedure of model training using the modified dataset by PCA.

Algorithm 1 Model training using samples modified by PCA [29]

Input: Training images $X = \{x | x \in [0, 1]^D\}$ and its covariance matrix C , training labels Y , and mean image \bar{x}
Parameters: Dimension of the PCA subspace d , dimension of additive noise m , noise scale $c > 0$, and desired model structure s

Output: Trained model with modified dataset.

- 1: Define a set of modified images $X' \leftarrow \{\}$.
 - 2: Perform spectral decomposition on C .

$$C = \sum_{i=1}^D \lambda_i v_i v_i^\top, \quad \lambda_1 \geq \lambda_2 \geq \dots \geq \lambda_D.$$
 - 3: **for** $x \in X$ **do**
 Project $x - \bar{x}$ on the eigenvector space.
 4:
$$a \leftarrow V^\top (x - \bar{x}), \quad V = [v_1, v_2, \dots, v_D].$$

 Add noise to obtain $a' = [a'_1, a'_2, \dots, a'_D]$.
 5:
$$a'_i = \begin{cases} a_i, & 1 \leq i \leq d \\ c\sqrt{\lambda_i} \xi_i, & d+1 \leq i \leq d+m \\ 0, & \text{otherwise,} \end{cases}$$

 where $\xi_i \sim \mathcal{N}(0, 1)$.
 Reconstruct modified image x' .
 6:
$$x' \leftarrow V a' + \bar{x}.$$

 7: Add x' to X' .
 8: **end for**
 9: Train s with X' to obtain the trained model.
-

Figure 9 shows the performance of the method for VGG16. Here, both hyperparameters m and c are set to 10, and d vary among 500, 800, and 1000 (noted as PCA500, PCA800, and PCA1000 in the figure, respectively). Universal

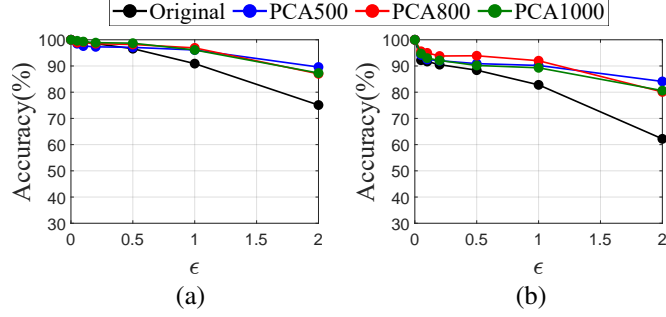


Figure 9: Classification accuracy of the original model and models trained using modified images. The amicable perturbations are found for `correctA` and applied to (a) `correctA` and (b) `correctB`.

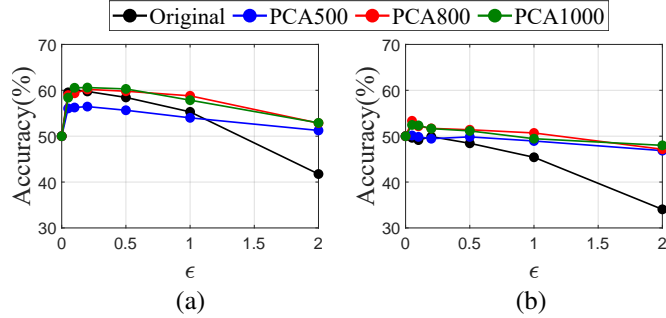


Figure 10: Classification accuracy of the original model and models trained using modified images. The amicable perturbations are found for `correctA+incorrectA` and applied to (a) `correctA+incorrectA` and (b) `correctB+incorrectB`.

perturbations are found from `correctA` and tested on both `correctA` and `correctB`. It is clearly observed that the models trained with the modified images show higher accuracy than the original model, demonstrating the improvement in finding universal amicable perturbations.

Figure 10 shows the performance of the data modification method when the universal perturbations are found from `correctA+incorrectA` and applied to `correctA+incorrectA` and `correctB+incorrectB`. Note that since the two datasets are combined, the default accuracy without aid is 50%. For the data used in finding universal perturbations, the accuracy is improved up to about 60% (Figure 10(a)). And, the accuracy for unseen data (`correctB+incorrectB`) effectively remains at 50% for a wide range of ϵ . Thus, even when both correctly classified images and incorrectly classified images are used, the method works as successfully as in the case when only correctly classified images are used.

5 Potential applications

Based on the results presented above, we discuss some potential applications where the amicable aid can be used.

Secure image communication. Consider a case where the sender wants to transmit an image to the receiver equipped with an image classifier but does not want an eavesdropper to identify the image content either visually or using a trained classifier. The strong aid can be used for secure image communication, since the strong aid can not only distort the image completely to prevent the eavesdropper from recognizing the content, but also the eavesdropper's classifier cannot correctly classify the strongly aided image due to its poor transferability.

Privacy-preserving image communication. Consider a cloud service where a personal image needs to be sent to the cloud server for classification and the result is returned to the user. This process may raise privacy concerns. Applying the strong aid can be a way to alleviate this issue, i.e., a strongly perturbed version of the image is sent to the server, which does not expose the image content, but the classification result can be still obtained. In this case, the universal aid would be practical so that a pre-computed perturbation can be immediately used at the user's device without knowledge of the classifier in the cloud server.

Protection against adversarial attacks. In Section 3.3, we showed that the aided image is more robust against attacks than the original image. Thus, the aid (especially the weak aid) can be applied as a protective measure against potential adversarial attacks. High transferability of the weak aid across models (Section 3.5) also supports the feasibility of this scenario.

6 Conclusion

We have introduced a new concept of the amicable aid that adds a perturbation to a given image in order to improve the classification performance for the image. We demonstrated that not only the weak aid with imperceptible perturbations but also the strong aid with perceptible perturbations are feasible. Furthermore, we showed that it is possible to obtain high-quality universal amicable perturbations by controlling the geometry of the decision boundary during training.

7 Limitation and future work

This paper presents the first study for the amicable aid, and opens new research directions for which much work needs to be performed in the future. (1) We presented one way to generate amicable perturbations, i.e., gradient-based off-manifold perturbations, but we believe that there are several other ways, e.g., on-manifold perturbations [30, 31], weight perturbations [32], etc. (2) We showed that strong amicable perturbations are not easily transferable across models, but it could be possible to improve their transferability, e.g., in a similar way to the approaches for improving transferability of adversarial attacks [33, 34]. (3) This paper focused on fundamental characteristics of the amicable aid with selected models and aid generation methods, but it will be desirable to perform large-scale benchmarking studies with more diverse models, datasets, and generation methods [35]. (4) Existence of adversarial perturbations have been shown for diverse tasks other than image classification [36, 37], and we believe that the same will apply to the amicable aid. (5) Actual implementation of the mentioned potential applications would be useful to demonstrate the practical value of the amicable aid beyond understanding of the working mechanisms of neural networks.

References

- [1] Dong Su, Huan Zhang, Hongge Chen, Jinfeng Yi, Pin-Yu Chen, and Yupeng Gao. Is robustness the cost of accuracy? – A comprehensive study on the robustness of 18 deep image classification models. In *Proceedings of the 15th European Conference on Computer Vision*, pages 631–648, 2018.
- [2] Ian J. Goodfellow, Jonathon Shlens, and Christian Szegedy. Explaining and harnessing adversarial examples. In *Proceedings of the 3rd International Conference on Learning Representations*, 2015.
- [3] Karen Simonyan and Andrew Zisserman. Very deep convolutional networks for large-scale image recognition. In *Proceedings of the 3rd International Conference on Learning Representations*, 2015.
- [4] Jaehui Hwang, Jun-Hyuk Kim, Jun-Ho Choi, and Jong-Seok Lee. Just one moment: Structural vulnerability of deep action recognition against one frame attack. In *Proceedings of the IEEE International Conference on Computer Vision*, pages 7668–7676, 2021.
- [5] Christian Szegedy, Wojciech Zaremba, Ilya Sutskever, Joan Bruna, Dumitru Erhan, Ian Goodfellow, and Rob Fergus. Intriguing properties of neural networks. In *Proceedings of the 2nd International Conference on Learning Representations*, 2014.
- [6] Alexey Kurakin, Ian Goodfellow, and Samy Bengio. Adversarial machine learning at scale. In *Proceedings of the 5th International Conference on Learning Representations*, 2017.
- [7] Nicholas Carlini and David Wagner. Towards evaluating the robustness of neural networks. In *Proceedings of the 38th IEEE Symposium on Security and Privacy*, pages 39–57, 2017.
- [8] Bo Luo, Yannan Liu, Lingxiao Wei, and Qiang Xu. Towards imperceptible and robust adversarial example attacks against neural networks. In *Proceedings of the 32nd AAAI Conference on Artificial Intelligence*, pages 1652–1659, 2018.
- [9] Aleksander Madry, Aleksandar Makelov, Ludwig Schmidt, Dimitris Tsipras, and Adrian Vladu. Towards deep learning models resistant to adversarial attacks. In *Proceedings of the 5th International Conference on Learning Representations*, pages 1–23, 2017.
- [10] Florian Tramèr, Alexey Kurakin, Nicolas Papernot, Ian Goodfellow, Dan Boneh, and Patrick McDaniel. Ensemble adversarial training: Attacks and defenses. *arXiv:1705.07204*, 2020.

- [11] Apostolos Modas, Seyed-Mohsen Moosavi-Dezfooli, and Pascal Frossard. SparseFool: a few pixels make a big difference. In *Proceedings of the 32nd IEEE Conference on Computer Vision and Pattern Recognition*, pages 9087–9096, 2019.
- [12] Eric Wong, Leslie Rice, and J Zico Kolter. Fast is better than free: Revisiting adversarial training. In *Proceedings of the 8th International Conference on Learning Representations*, pages 1–17, 2020.
- [13] Francesco Croce and Matthias Hein. Reliable evaluation of adversarial robustness with an ensemble of diverse parameter-free attacks. In *Proceedings of the 37th International Conference on Machine Learning*, pages 2206–2216, 2020.
- [14] Nicolas Papernot, Patrick McDaniel, Ian Goodfellow, Somesh Jha, Z. Berkay Celik, and Ananthram Swami. Practical black-box attacks against machine learning. In *Proceedings of the ACM Asia Conference on Computer and Communications Security*, 2017.
- [15] Yandong Li, Lijun Li, Liqiang Wang, Tong Zhang, and Boqing Gong. Nattack: Learning the distributions of adversarial examples for an improved black-box attack on deep neural networks. In *Proceedings of the International Conference on Machine Learning*, 2019.
- [16] Seyed-Mohsen Moosavi-Dezfooli, Alhussein Fawzi, Omar Fawzi, and Pascal Frossard. Universal adversarial perturbations. In *Proceedings of the 30th IEEE Conference on Computer Vision and Pattern Recognition*, pages 1765–1773, 2017.
- [17] David Stutz, Matthias Hein, and Bernt Schiele. Disentangling adversarial robustness and generalization. In *Proceedings of the 32nd IEEE Conference on Computer Vision and Pattern Recognition*, pages 6976–6987, 2019.
- [18] Yang Song, Rui Shu, Nate Kushman, and Stefano Ermon. Constructing unrestricted adversarial examples with generative models. In *Advances in Neural Information Processing Systems*, 2018.
- [19] Thomas Tanay and Lewis Griffin. A boundary tilting perspective on the phenomenon of adversarial examples. *arXiv:1608.07690*, 2016.
- [20] Nils Lukas, Yuxuan Zhang, and Florian Kerschbaum. Deep neural network fingerprinting by conferrable adversarial examples. In *Proceedings of the 9th International Conference on Learning Representations*, pages 1–18, 2021.
- [21] Cihang Xie, Mingxing Tan, Boqing Gong, Jiang Wang, Alan L. Yuille, and Quoc V. Le. Adversarial examples improve image recognition. In *Proceedings of the 33rd IEEE Conference on Computer Vision and Pattern Recognition*, pages 819–828, 2020.
- [22] Mohammad A. A. K. Jalwana, Naveed Akhtar, Mohammed Bennamoun, and Ajmal Mian. Attack to explain deep representation. In *Proceedings of the 33rd IEEE Conference on Computer Vision and Pattern Recognition*, pages 9543–9552, 2020.
- [23] Hanxun Huang, Xingjun Ma, Sarah Monazam Erfani, James Bailey, and Yisen Wang. Unlearnable examples: Making personal data unexploitable. In *Proceedings of the 9th International Conference on Learning Representations*, pages 1–17, 2021.
- [24] Alex Krizhevsky. Learning multiple layers of features from tiny images, 2009.
- [25] Kaiming He, Xiangyu Zhang, Shaoqing Ren, and Jian Sun. Deep residual learning for image recognition. In *Proceedings of the 29th IEEE Conference on Computer Vision and Pattern Recognition*, 2016.
- [26] Mark Sandler, Andrew Howard, Menglong Zhu, Andrey Zhmoginov, and Liang-Chieh Chen. MobileNetV2: Inverted residuals and linear bottlenecks. In *Proceedings of the 31st IEEE Conference on Computer Vision and Pattern Recognition*, 2018.
- [27] Ramprasaath R. Selvaraju, Michael Cogswell, Abhishek Das, Ramakrishna Vedantam, Devi Parikh, and Dhruv Batra. Grad-CAM: Visual explanations from deep networks via gradient-based localization. *International Journal of Computer Vision*, 128(2):336–359, 2019.
- [28] Yanpei Liu, Xinyun Chen, Chang Liu, and Dawn Song. Delving into transferable adversarial examples and black-box attacks. In *Proceedings of the International Conference on Learning Representations*, 2016.
- [29] Yueru Li, Shuyu Cheng, Hang Su, and Jun Zhu. Defense against adversarial attacks via controlling gradient leaking on embedded manifolds. In *Proceedings of the 16th European Conference on Computer Vision*, pages 753–769, 2020.
- [30] Ali Shahin Shamsabadi, Ricardo Sanchez-Matilla, and Andrea Cavallaro. ColorFool: Semantic adversarial colorization. In *Proceedings of the IEEE Conference on Computer Vision and Pattern Recognition*, pages 1151–1160, 2020.

- [31] Zhengyu Zhao, Zhuoran Liu, and Martha Larson. Towards large yet imperceptible adversarial image perturbations with perceptual color distance. In *Proceedings of the IEEE Conference on Computer Vision and Pattern Recognition*, pages 1039–1048, 2020.
- [32] Jiawang Bai, Baoyuan Wu, Yong Zhang, Yiming Li, Zhifeng Li, and Shu-Tao Xia. Targeted attack against deep neural networks via flipping limited weight bits. In *Proceedings of the International Conference on Learning Representations*, 2021.
- [33] Weibin Wu, Yuxin Su, Michael R. Lyu, and Irwin King. Improving the transferability of adversarial samples with adversarial transformations. In *Proceedings of the Conference on Computer Vision and Pattern Recognition*, pages 9024–9033, 2021.
- [34] Xiaosen Wang and Kun He. Enhancing the transferability of adversarial attacks through variance tuning. In *Proceedings of the Conference on Computer Vision and Pattern Recognition*, pages 1924–1933, 2021.
- [35] Yinpeng Dong, Qi-An Fu, Xiao Yang, Tianyu Pang, Hang Su, Zihao Xiao, and Jun Zhu. Benchmarking adversarial robustness on image classification. In *Proceedings of the IEEE Conference on Computer Vision and Pattern Recognition*, pages 321–331, 2020.
- [36] Cihang Xie, Jianyu Wang, Zhishuai Zhang, Yuyin Zhou, Lingxi Xie, and Alan Yuille. Adversarial examples for semantic segmentation and object detection. In *Proceedings of the International Conference on Computer Vision*, pages 1369–1378, 2017.
- [37] Jun-Ho Choi, Huan Zhang, Jun-Hyuk Kim, Cho-Jui Hsieh, and Jong-Seok Lee. Evaluating robustness of deep image super-resolution against adversarial attacks. In *Proceedings of the International Conference on Computer Vision*, pages 303–311, 2019.
- [38] Alexey Kurakin, Ian Goodfellow, Samy Bengio, Yinpeng Dong, Fangzhou Liao, Ming Liang, Tianyu Pang, Jun Zhu, Xiaolin Hu, Cihang Xie, Jianyu Wang, Zhishuai Zhang, Zhou Ren, Alan Yuille, Sangxia Huang, Yao Zhao, Yuzhe Zhao, Zhonglin Han, Junjiajia Long, Yerkebulan Berdibekov, Takuya Akiba, Seiya Tokui, and Motoki Abe. Adversarial attacks and defences competition. *arXiv:1804.00097*, 2018.
- [39] Diederik P. Kingma and Jimmy Ba. Adam: A method for stochastic optimization. In *Proceedings of the International Conference on Learning Representations*, 2015.

A Results on additional dataset

In Section 3.1 of the main paper, we observed the efficacy of the amicable aid on the CIFAR-100 dataset. Here, we explore if the amicable aid also works well for an additional dataset, namely, the NIPS 2017 Adversarial Attacks and Defenses Competition dataset [38]² containing 1,000 images having a resolution of 299×299 pixels. As in Section 3.1 of the main paper, VGG16, ResNet50, and MobileNetV2 are employed, which are pre-trained on ImageNet, and we set $\epsilon = .05$ for the weak amicable aid or $\epsilon = 5$ for the strong amicable aid with a number of iterations of $N = 50$ in both cases. The results are shown in Table 4. It is observed that the amicable aid can improve the classification performance on this dataset as in the case of CIFAR-100.

Table 4: Classification accuracy (with average confidence for the true class labels) for the original images, weakly aided images, and strongly aided images for the NIPS 2017 Adversarial Attacks and Defenses Competition dataset.

	VGG16	ResNet50	MobileNetV2
Original	80.80% (.6928)	93.20% (.8222)	89.00% (.7329)
Weak aid	98.90% (.9865)	100.0% (.9996)	100.0% (1.000)
Strong aid	96.70% (.9666)	98.00% (.9808)	99.70% (.9915)

B Amicable aid based on C&W

In the main paper, we developed the amicable aid based on I-FGSM. However, other gradient-based adversarial attack methods can be also used to perform the amicable aid. Here, we show the results of the amicable aid formulated in a similar way to the C&W adversarial attack method [7]. We formulate the amicable aid based on C&W as the following optimization problem.

$$\min_{\delta} \|\delta\|_2 + c \cdot f(x + \delta) \quad (6)$$

$$\text{such that } x + \delta \in [0, 1]^D, \quad (7)$$

where x is the given image, δ is the perturbation, c is a hyperparameter, and D is the dimension of x . f is given by

$$f(x) = \max \mathcal{C}(x) - \mathcal{C}(x)_y, \quad (8)$$

where \mathcal{C} is the classifier and $\mathcal{C}(x)_y$ is the classifier's output (probability) for the true class label y . We solve this optimization problem using the Adam optimizer [39] with a learning rate of .01. We use $c = 1$ for the weak aid and $c = 10000$ for the strong aid, which are experimentally determined. The results using VGG16 for the CIFAR-100 dataset are shown in Table 5, which demonstrate that the amicable aid can be successfully designed based on the C&W attack method. Figure 11 depicts example images to compare the images aided by the method in the main paper (based on I-FGSM) and the C&W-based method. In both methods, the weakly aided images have almost no difference from the original ones, while the strongly aided images hardly preserve the original content. However, the distorted images by the strong aid are visually different between the two methods. This is because the aid based on I-FGSM uses the l_{∞} -norm while the aid based on C&W uses the l_2 -norm. Furthermore, our formulation of the C&W-based aid does not necessarily increase the confidence score for a correctly classified image (the first row in Figure 11) because f in (8) becomes 0 for such an image.

C Improving universal aid for other models

Section 4.2 of the main paper showed the effectiveness of the image modification method using PCA for improving the universal aid when the VGG16 structure is used. We apply the same method for the other two model structures, ResNet50 and MobileNetV2, and the results are shown in Figures 12 and 13, respectively. The trend in these figures are similar to those in Figures 9 and 10 of the main paper, indicating that the image modification method using PCA works for all the tested models.

²<https://kaggle.com/c/6864>

Table 5: Classification accuracy (with average confidence for the true class labels) for the original images, weakly aided images, and strongly aided images for CIFAR-100 when VGG16 is employed.

	Original	Weak aid	Strong aid
Accuracy	72.32%	97.82%	99.96%
Confidence	.7090	.8584	.6977

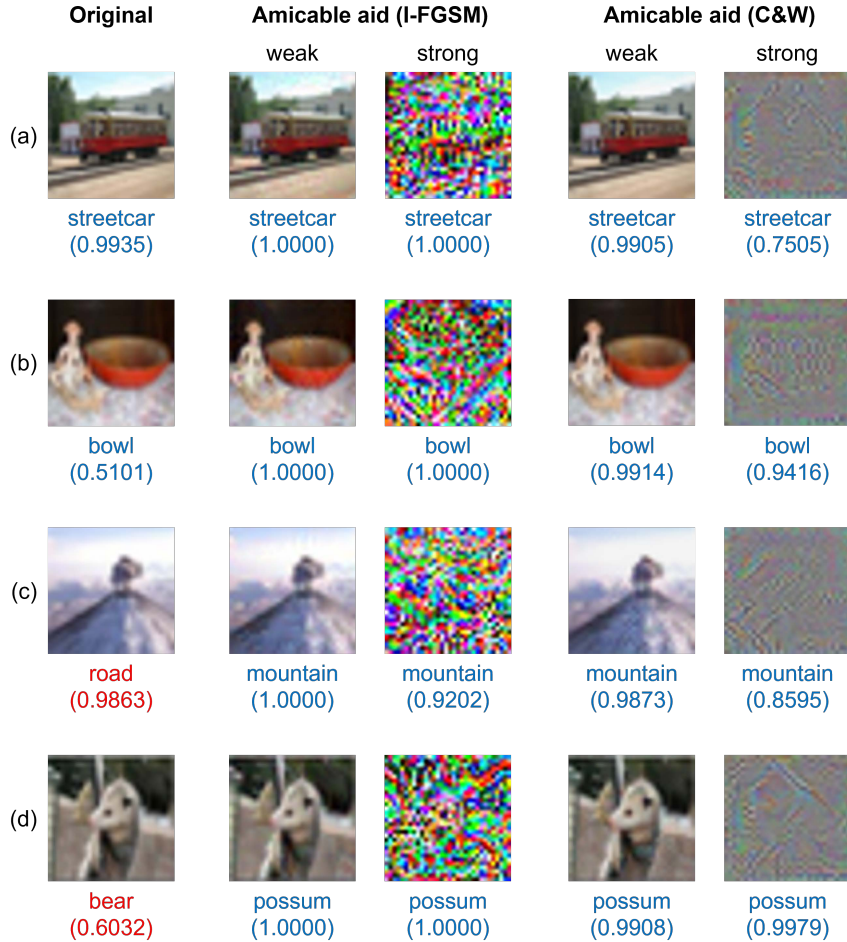


Figure 11: Comparison of the amicable aid based on I-FGSM and C&W. The original images in (a) and (b) are correctly classified and their aided versions are also correctly classified. The original images in (c) and (d) are misclassified, but their aided versions are correctly classified.

D Model training

The models for CIFAR-100 were trained with the following parameters. The cross-entropy loss was minimized using the SGD optimizer for 200 epochs with an initial learning rate of 0.1, a momentum parameter of 0.9, and a weight decay parameter of .0005.

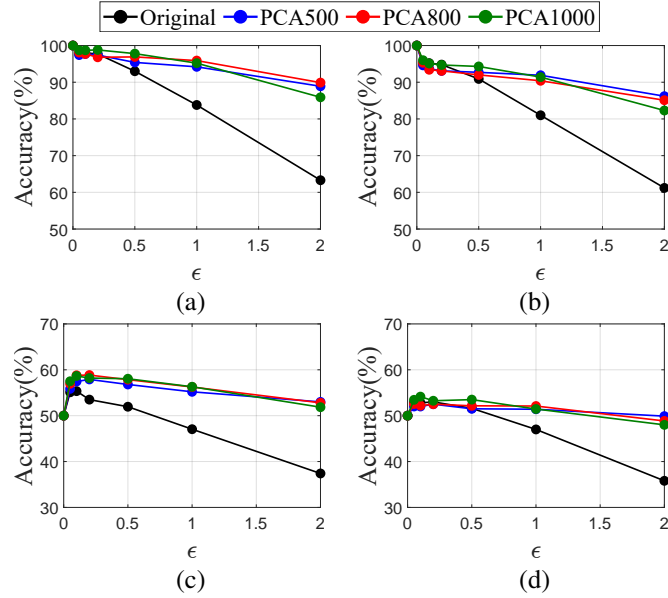


Figure 12: Classification accuracy of the original model and the models trained using modified images when ResNet50 is used. The amicable perturbations are found for `correctA` and applied to (a) `correctA` and (b) `correctB`, or for `correctA+incorrectA` and applied to (c) `correctA+incorrectA` and (d) `correctB+incorrectB`.

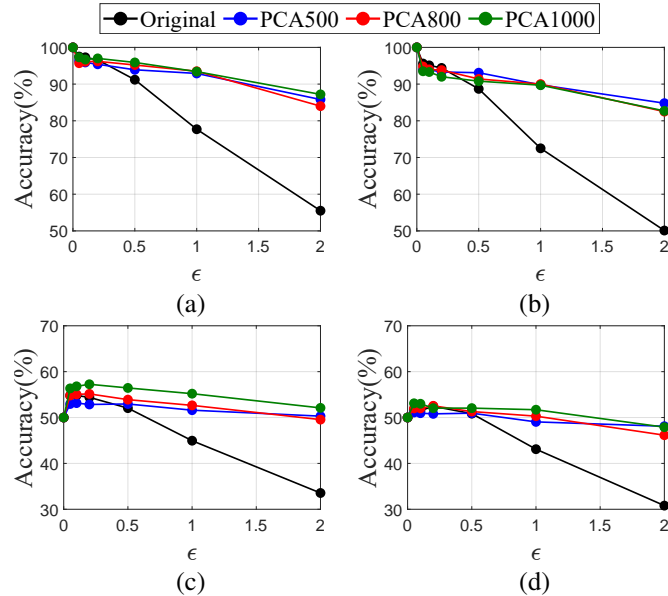


Figure 13: Classification accuracy of the original model and the models trained using modified images when MobileNetV2 is used. The amicable perturbations are found for `correctA` and applied to (a) `correctA` and (b) `correctB`, or for `correctA+incorrectA` and applied to (c) `correctA+incorrectA` and (d) `correctB+incorrectB`.